Ultrasonic device for measuring periodontal attachment levels

J. E. Lynch and M. K. Hinders
Department of Applied Science, College of William and Mary, P. O. Box 8795, Williamsburg, Virginia 23187

(Received 18 June 2001; accepted for publication 11 April 2002)

Periodontal disease is manifested clinically by a degradation of the ligament that attaches the tooth to the bone. The most widely used diagnostic tool for assessment of periodontal diseases, measurement of periodontal attachment loss with a manual probe, may overestimate attachment loss by as much as 2 mm in untreated sites, while underestimating attachment loss by an even greater margin following treatment. Manual probing is also invasive, which causes patient discomfort. This work describes the development and testing of an ultrasonographic periodontal probe designed to replace manual probing. It uses a thin stream of water to project an ultrasonic beam into the periodontal pocket, and then measures echoes off features within the pocket. To do so, the ultrasonic beam must be narrowed from 2 (the diameter of the transducer) to 0.5 mm (the approximate width of the periodontal pocket at the gingival margin). The proper choice of transducer frequency, the proper method for controlling water flow from the probe, and a model for interpreting these echoes are also addressed. Initial results indicate that the device measures echoes from the hard tissue of the tooth surface, and that the periodontal attachment level can be inferred from these echoes. © *2002 American Institute of Physics.* [DOI: 10.1063/1.1484235]

I. INTRODUCTION

Periodontal disease is one of the two major causes of tooth loss today, and is widely pervasive in older adults. Despite the widespread problem of periodontal disease today, currently available diagnostic tests are limited in their effectiveness.[1] The best available diagnostic aid, probing pocket depths, is only a retrospective analysis of attachment already lost.[2–8] In this technique, a probe is placed between the soft tissue of the gingival margin and the tooth. Using fixed markings on the probe, typically 1 or 2 mm apart, the depth of probe penetration is measured relative to a fixed point on the tooth such as the cemento-enamel junction (where the enamel ends) called the clinical attachment level. Alternatively, the depth is measured relative to the gingival margin (gum line) called the probing depth.

Numerous studies have questioned the ability of the periodontal probe to accurately measure the anatomic pocket depth.[9–12] Instead, the periodontal probe measures the probing attachment level, which is defined as the distance from the cemento-enamel junction to the apical depth of periodontal probe tip penetration into the gingival crevice. The degree of probe tip penetration may be influenced by factors such as thickness of the probe, pressure applied, tooth contour, tooth position, presence of calculus, degree of periodontal inflammation, and the actual level of connective tissue fibers.[13–18]

As a result, probing measurements may overestimate attachment loss by as much as 2 mm in untreated sites, while underestimating attachment loss by an even greater margin following treatment.[19,20] The development of automated, controlled force probes has reduced some of the operator-related error and subjectivity inherent in manual probing techniques.[21–24] However, standardized probing forces do not address anatomic and inflammatory factors.[25–27]

In addition, a computer-vision system that automates the reading of manual probe marking to the nearest 0.1 mm has been investigated to improve the accuracy of the depth readings.[28,29] Once again, this technique only addresses one concern associated with manual probing—the inaccuracy in reading probing depths—while failing to address other sources of error.

Due to the inherent measurement error of routine manual probing, a 2 to 3 mm loss of probing attachment is required before a statistically significant loss of actual connective tissue can be identified.[30,31] A manual probe cannot accurately detect small changes in attachment level until the cumulative loss reaches this threshold. The accuracy of research-oriented, computerized controlled force probes reduces this critical attachment loss threshold to a potential minimum of ± 1 mm.[32]

Subtraction radiography provides an alternative to manual probing. However, it can only measure loss of the supporting aveolar bone, which lags losses in connective tissue by several months.[33–37] Also, serial radiography subjects patients to increasing amounts of ionizing radiation, so that its use is limited to patients who have already been identified as at risk for periodontal disease.

As an alternative to these diagnostic tests, an ultrasonic device has been developed that uses a small amount of water to couple the ultrasound wave into the pocket space. A tip placed over the transducer narrows the ultrasonic beam to approximately the same width as the opening into the sulcus at the gingival margin.

II. SYSTEM DESIGN

The ultrasonic probe was designed to have a removable tip, room for a 2 mm active area transducer housed at the base of this tip, a water line input running through the probe handle and emptying into a small open area around the trans-

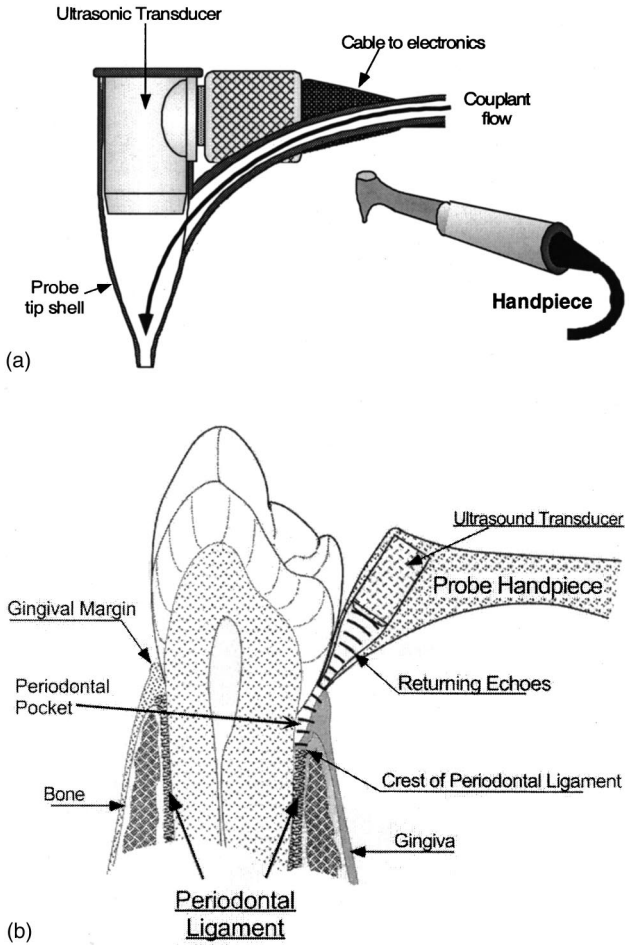

FIG. 1. A schematic of (a) the ultrasonic periodontal probe as well as (b) the typical anatomy of dentition and probe position.

ducer, and an electronics input–output cable also running through the base and connected to the transducer (Fig. 1).

The transducer was driven using the Matec SR-9000 pulser-receiver card, which is a plug-in card designed to connect to a 16-bit expansion slot in an IBM-compatible computer. The pulser produces a unipolar spike pulse with a voltage output of up to 300 V and a rise time of less than 10 ns into a 50 Ω cable. The receiver offers 63.5 dB of computer addressable gain in 0.5 dB steps and has a bandwidth of 50 MHz (with a low frequency end of 100 kHz). In addition, the receiver has independently adjustable low-pass and high-pass filters. The low-pass filter was set to full band, while the high-pass filter was set to 7.5 MHz to filter out low frequency noise.

The receiver output was connected to a Gage CompuScope 2125 analog-to-digital converter. The digitized signal was processed and saved using programs running LabView version 5.0. This system was run using a rackmount-type computer with a Pentium Pro processor contained in a ruggedized, portable case.

The water line between the handpiece and the water source was equipped with a low-pressure regulating valve from Beaverstate Dental. This valve reduced the input water line pressure of up to 250 psi down to an adjustable range of 2–30 psi. After a systematic investigation of the return signal at various pressure settings, it was determined that a pressure setting below 5 psi provides the laminar flow needed for accurate imaging with the periodontal probe.

Finally, a range of custom transducers with a 2-mm-diam active area, a center frequency ranging from 10–25 MHz, and −6 dB bandwidth of between 5 and 8 MHz, were produced by Valpey–Fisher, Inc., and tested for use in this probe. As a general rule, the higher frequency transducers required more damping to eliminate ringing in the signal, caused by secondary vibrations in the transducer. So although higher frequency signals are theoretically capable of greater axial resolution, ringing reduced the effective resolution. Ringing can be eliminated through greater damping of the transducer, but only by sacrificing signal strength.

As a result, the 20 and 25 MHz transducers did not provide enough signal strength to image small structures adequately, while the 10 and 15 MHz transducers provided comparable resolution and signal strength. In addition, two other manufacturers provided 15 and 20 MHz custom transducers that did not perform well enough to use in this comparison study. Therefore, the 10 MHz transducers were used in the tests that follow. Although the 15 MHz transducers performed equally well in the study, the 10 MHz transducers are easier to obtain, since 2-mm-diam transducers that operate above 10 MHz are difficult to produce.

III. DETERMINATION OF OPTIMAL TIP SHAPE

A key component of the ultrasonic periodontal probe is the hollow funnel-shaped tip that houses the ultrasound transducer. This tip narrows the beam path of the ultrasound wave, thereby allowing it to enter the periodontal pocket without scattering. Because the tip alters the shape of the ultrasonic beam, the design of this tip has a large impact on the performance of the periodontal probe.

To determine what tip shape produces the strongest and least-distorted return signal, a computer simulation was developed using the cylindrical acoustic finite integration technique (CAFIT), which is based on finite volume integration, a special formulation of the finite difference method of computing the solution to differential equations.[38]

The CAFIT algorithm is employed on a staggered grid, with the pressure elements a half-unit apart from the r and z direction velocity elements. The staggered grid provides a better physical representation of the pressure field, since staggering gives a more accurate representation of nonuniform pressure gradients.[39] In addition, the staggered grid provides better accuracy with less calculation time than second-order finite difference techniques, because it effectively divides the spatial lattice in half without requiring a corresponding halving of time steps to satisfy the Courant condition for numeric stability.

The CAFIT algorithm was first implemented for a conical tip with walls sloping down to a narrow opening, 0.5 reduced units (r.u.) in diameter. In this simulation, the reduced unit for distance is 1 r.u.=1 mm and for time, 1 r.u. is the time it takes to move 1 r.u. of distance at the speed of sound in water, 1480 m/s. The top of the tip was 4.0 r.u. in diameter with a 2.0 r.u. diameter transducer placed in the middle of this area. To set the boundary conditions, the walls

of the tip were assumed to be completely rigid, while outside the tip the vacuum boundary condition was used at the air/water interface. Finally, the simulation was set up so that the probe was aimed at a metal reflector 20 mm from the transducer face, and an input wave pulse of the form $\sin(2\pi ft)*\sin(0.2\pi ft)$ that lasted 0.5 r.u. was sent down the tip.

After confirming the stability of this algorithm for $\Delta r \leqslant 0.005$, the simulation was run on a range of tip geometries to determine which would produce the strongest output signal for the periodontal probe.

First, the angle θ of the tip walls was varied from 0° to 90° in 5° increments, and the strongest return peaks occurred for the 80° and 85° angles. These angles correspond to a smooth slope from the outer diameter at the top of the nozzle to the tip outlet at the bottom.

Next, the diameter of the nozzle at the top was varied from 2 (the nozzle touching the edge of the transducer) to 6 r.u., for a wall smoothly sloping down to the tip outlet. The strongest return peak occurred when the nozzle diameter was 2 r.u. and the peak decreased as the diameter increased.

Thus, to optimize tip performance, its top diameter should conform as close as possible to the transducer diameter, while making it as long as possible so that the angle θ is as close to 90° as possible. Such a design minimizes the area of the tip wall perpendicular to the wavefront.

While minimizing the top diameter and maximizing the wall angle are useful guidelines for designing the tip, there are some practical limitations to these goals. First, the nozzle top needs to be a little wider than the transducer face to accommodate transducer packaging, and to allow adequate room for coupling water to flow into the tip. Second, the tip length cannot be too long, because it must fit comfortably in the patient's mouth.

After examining these general relationships, a few specific shapes were considered, including:

(1) One where the radius of the tip walls varied exponentially: $r=r_i e^{-mz}$.
(2) One where the radius of the tip walls takes a parabolic shape: $z=(r-r_i)^2+c^2$.
(3) One where the radius of the tip walls takes an ellipsoid shape: $z^2+(r-r_i)2=c^2$.
(4) One where the radius of the tip walls takes a spline shape.

In the simulation, the exponential walls produced the strongest return signal, although only slightly better than the linear walls. Because the exponential walls narrow more quickly, they confine the waveform before it has time to spread out. However, further down the walls, the curved edges of the exponential walls have more area perpendicular to the wavefront than the linear tip, thereby causing internal reflections.

Based on these results, a linear tip that has a slight ''nook'' at the top was fabricated that incorporates the best features of the exponential and the linear tips. For the purposes of complete experimental validation, an exponential tip, a spline-shaped tip, and a linear tip without the nook were also fabricated (Fig. 2).

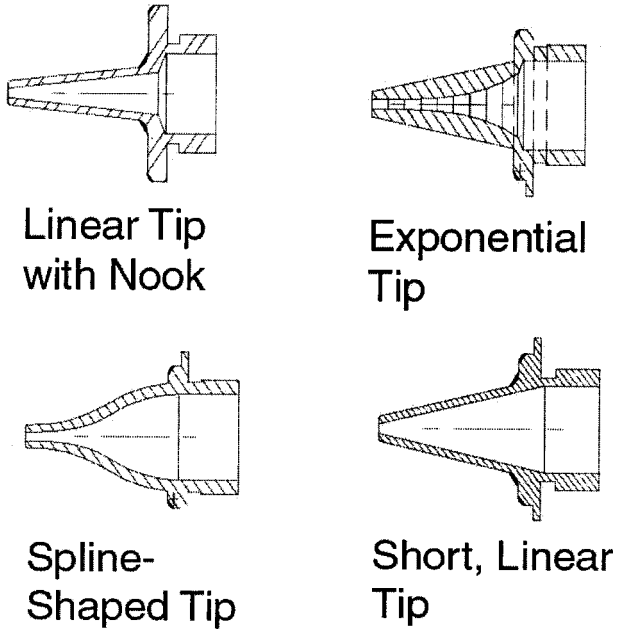

FIG. 2. The tips produced for testing with the ultrasonic probe.

After making these tips, the periodontal probe was aimed at a flat metal target 20 mm away from the transducer face, thus recreating the conditions of the simulations. In the simulation, the long, thin linear tip (with the short nook at the top) produced the strongest return signal, followed by the exponential tip, the shorter linear tip, and then the spline-shaped tips walls. The experiment, however, showed that the two linear tips performed the best, while the exponential and spline-shaped tips hardly produced a return at all. This difference between the simulation predictions and the experimental results could be because the exponential and spline-shaped tips produce most of their backscatter up within the tip. Because real signals attenuate, earlier scattering has a disproportionate effect on the size of the return signal (Fig. 3).

One factor possibly contributing to the difference may lie in the technique used to fabricate the tips. The first three tips (thin linear, exponential, and spline-shaped) were made by step-drilling a rough outline of the shape, followed by a finer cut using electrodischarge machining (EDM). The process was completed by polishing the inside with a fine grit. While this process produced tips of acceptable quality, it was very difficult to reproduce, primarily because it was difficult to center the EDM electrode with the step-drilled holes. Also, the exponential and spline-shaped tips are more complicated shapes, possibly leading to significant manufacturing irregularities that are hard to inspect.

Due to these problems with EDM fabrication, a second manufacturing technique was tested with the second, shorter linear tip. In this technique, a conical reamer was produced to drill out the hole for the linear sloping tip. The reamer can only produce very simple shapes, like the short, linear tip (which, in contrast to the longer linear tip, does not have a small nook at the top of the tip). This process produced per-

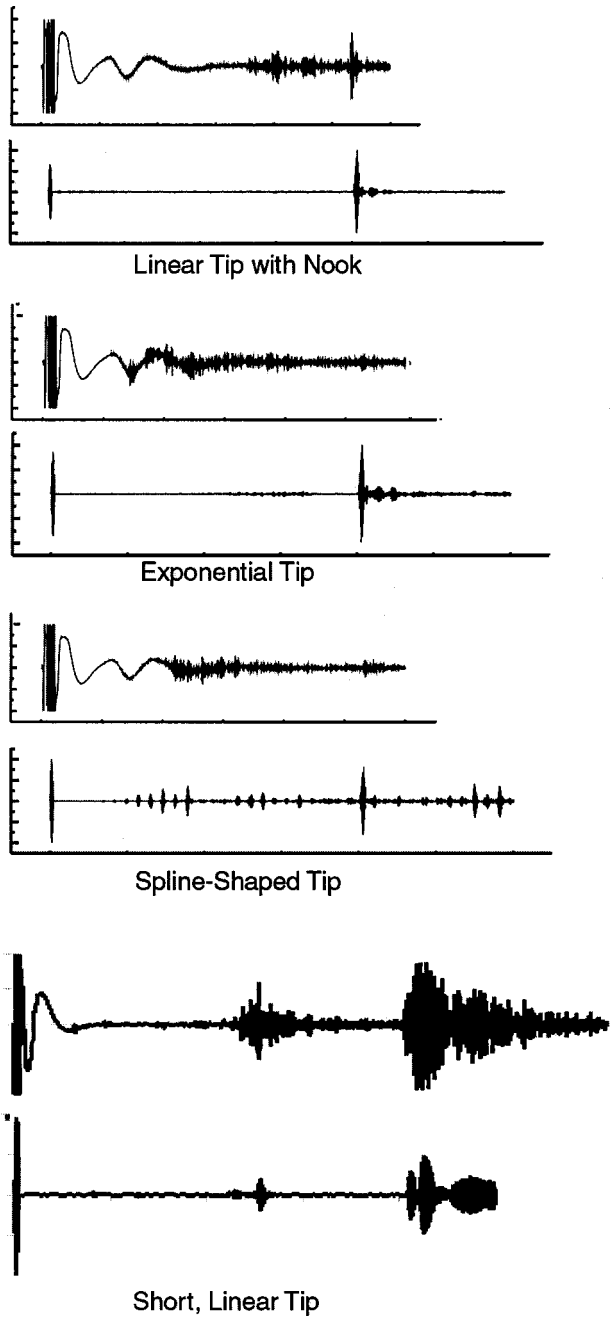

FIG. 3. A comparison of the experimental (top) vs simulated (bottom) results for each of the tip shapes tested.

fectly aligned holes, but also left grooves along the walls as an artifact of the drilling. These grooves were too deep to remove through polishing, and they produced significant reflections that made these tips unusable.

To remove these grooves, the same shape tips were made by this process out of brass rather than stainless steel, and the grooves were etched using a bath of nitric acid. This etching removed the grooves, resulting in the tips used in the comparisons above.

Therefore, both the CAFIT simulation and the experimental evidence indicate that linear tip walls sloping down to a narrow outlet reduce the ultrasonic beam profile with the least scattering. In addition, a sharper slope early on (before the wave has spread out too much to reflect off these sharply sloping walls) produces the narrowest orifice towards the end of the tip, further improving the signal output.

IV. PRELIMINARY TESTS

After the prototype ultrasonic periodontal probe was completed, a series of tests was conducted to determine how effective the probe was at measuring the depth of periodontal pockets, and to begin developing methods for analyzing the return signals.

The first test was conducted on a human subject, in which a single ultrasonic A scan of the periodontal pocket was saved. In this setup, a dental hygienist held the probe while an operator viewed the oscilloscope trace on the custom LabView data acquisition software's graphical user interface. As the hygienist pivoted the probe through various angles, the operator viewed which trace provided the best return signals and told the hygienist to hold the probe in place to save that oscilloscope trace.

This process was repeated on three different pockets chosen for their pocket depths as measured with a manual periodontal probe. One pocket depth was 3 mm, one 4 mm, and one 5 mm. For each pocket, two sets of ultrasonic probing measurements were taken, once of a single trace and once of a trace averaged from 50 continuously acquired signals.

This process proved to be cumbersome, since the return signal would fade as the probe angle changed slightly due to hand jiggle, or as variations in water flow slightly changed the return signal. In addition, signal averaging resulting in blurring of the return signal, which is evidence that the signal is not stationary but evolves over time.

To eliminate the coordination problems between saving a trace and properly orienting the probe, the Lab View data acquisition software was modified to continuously save a series of scans as the hygienist aimed the probe in the periodontal pocket. In later tests using the modified software, the probe started out in a vertical position, nearly parallel to the tooth face. From this position, the hygienist slightly moved the probe about its vertical axis while watching the display to see if slight changes in probe position would provide a stronger return signal. However, after looking at a few teeth the strongest signal always came from the starting position, and so the hygienist was instructed not to move the probe from that position.

After obtaining these data, the digitized A scans were transferred to another computer for later analysis. Each trace was visually inspected to determine pockets depths as a time delay between the obvious tip echoes and the more subtle pocket-bottom echoes. These measurements were compared to the pocket depths measured with the manual probe by normalizing with the speed of sound in water, 1480 m/s. Because the probe tip was placed at the gum line, the zero reference on the ultrasonic echo traces corresponded directly to the manual probing zero references.

Because the ultrasonic scans produce such a cluttered signal, a visual examination is a laborious and subjective measurement. The eye must pick out which peak among many is the feature of interest, and visually determine its

position. Training a dental hygienist to make such a complicated interpretation of the data in a clinical setting is highly unrealistic given the short time allowed for the probing and the myriad other duties of the hygienist. In cardiology and obstetrics, by contrast, highly specialized sonographers are available to both perform ultrasound examinations and do some of the interpretations for the physicians. Any practical tool for ultrasonically measuring periodontal pockets depths in the general dentistry office must be able to automatically extract the feature of interest from the ultrasonic echoes without depending on the presence of an ultrasound expert.

The first step in automating this data analysis is to simplify the trace and isolate only the features of interest. To this end, an automated pick-peaking algorithm widely used in making spectrographic measurements was adapted for this analysis. The slope-detection algorithm used in this project was modified from a commercial routine freely available from Galactic Industries Corp.[40] In this algorithm, the first derivative of the discrete waveform is taken using a central difference approximation, and the average value of the first derivative is computed. Next, the local maxima are found wherever the derivative changes sign from positive to negative. If the slope just before this point is greater than the average slope, the original value of that data point is retained. All other points are set to zero.

The next step is to smooth the data by taking the maximum value within each block of 10 data points. Data smoothing reduces resolution between scan points from 0.0075 to 0.075 mm, which is still smaller than the fundamental axial resolution limit for a 10 MHz transducer.

This simplified waveform can be further improved by averaging the traces acquired while holding the probe in one position. While averaging tended to blur the original signal, peak picking and smoothing eliminates small variations in the signal due to movement of the probe, changes in water flow, or other factors. A comparison of the original waveform to the waveform after this processing has been completed can be seen in Fig. 4.

After this processing was performed, a second comparison of manual probing depths to the processed data was performed, which produced more accurate results than the analysis of the raw data, as can be seen in Fig. 5.

While peak detection followed by signal averaging simplifies the waveform and improves pocket-depth measurement accuracy, some human interpretation of the data is still required. However, with more clinical data, it is hoped that the peak-picking algorithm can be combined with a fully automated signal-interpretation algorithm.

V. DISCUSSION

The ultrasonic periodontal probe described here has been demonstrated to measure echoes from the periodontal pocket, and a signal processing routine has been proposed to aid in the interpretation of these echoes.

However, if this probe is to replace manual probing as the new standard for the diagnosis of periodontal disease, a more detailed understanding of the origin of these echoes is needed. Correlating the echoes to manual probing is not an entirely satisfying approach, due to the inherent inaccuracy of the manual probe. In addition, manual probing measures resistance to probing force within the periodontal pocket, not the depth of a specific anatomic feature.

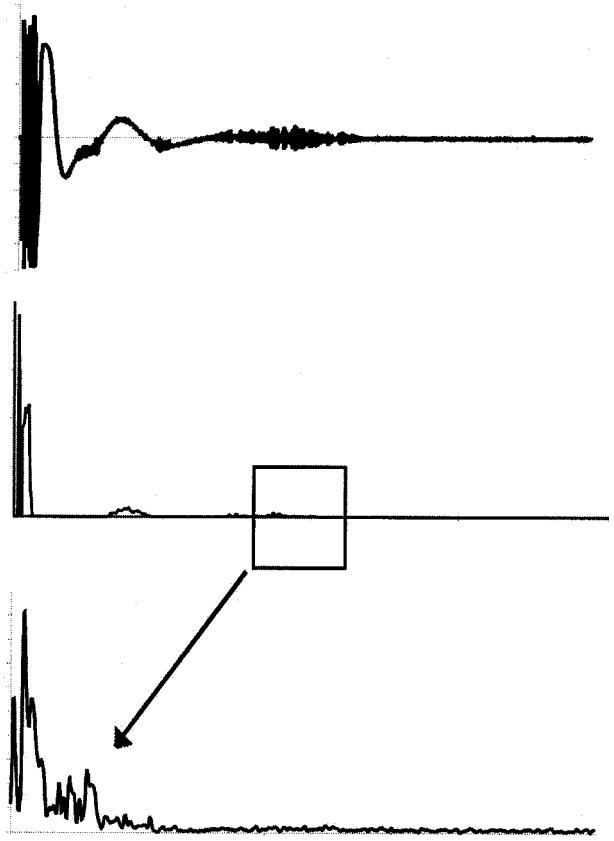

FIG. 4. A comparison of the return signal trace from the periodontal pocket before (top) and after (middle) signal processing. The bottom trace zooms in on the region of the processed waveform that corresponds to the area from the tip outlet to the periodontal pocket.

Therefore, future clinical studies will need to be conducted that will allow comparisons to anatomic features in the periodontal pocket. Flap surgery (when the gum line is opened to allow removal of plaque and calculus in patients with severe periodontal disease), en bloc surgery (when a cancerous section of the jaw is removed), and extracted teeth studies are three possible procedures that will allow such a comparison.

To help guide the interpretation of the data obtained in these future studies, a candidate model describing ultrasonic wave propagation within the periodontium has been developed. This model is based on two observations. First, in one test a patient had very smooth teeth due to a loss of enamel, which led to weak ultrasonographic return signals. Second, probing sites with unusually strong signals indicated correlation with teeth with ''alot of anatomy,'' or surface irregularities that produced ultrasonic returns. Based on these observations, the first assumption of the model is that signals analyzed using the probe are composed entirely of echoes off hard tissue within the periodontium.

Although the signal is composed from echoes off hard tissues, rather than the soft tissues really of interest, these data can be used to infer the depth of the periodontal pocket.

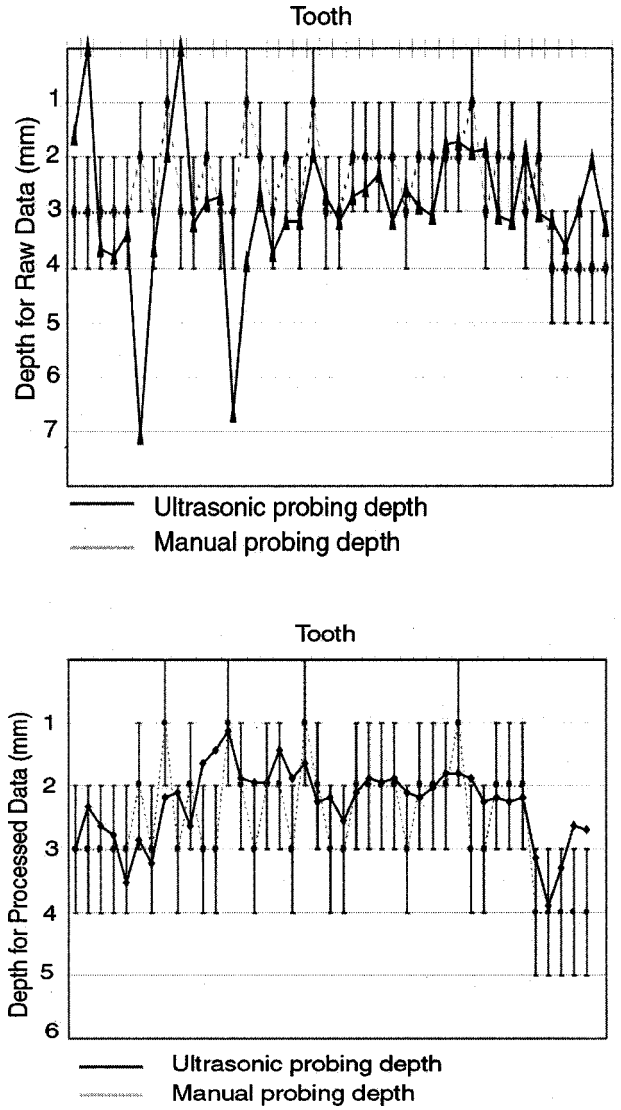

FIG. 5. A comparison of manual probing depths and the position where the ultrasonic signal ends for the raw ultrasonic signal (top) and the signal after processing (bottom).

Within the pocket, the surface of the tooth is exposed, and ultrasonic signals can echo directly off the tooth surface. However, if the tooth surface is covered with tissue, the echo will be attenuated. Because the junctional epithelium (thin layer of attached gum tissue) is softer and less heterogeneous than the connective tissue, it is reasonable to assume that it will attenuate the signal less than the fibrous, and hence highly scattering, connective tissue. This leads to the three regions within the return signal:

(1) A near region of very strong returns, in which the ultrasonic wave passes through water (from the probe) to echo off the tooth surface.
(2) A middle region of slightly attenuated returns, in which the ultrasonic wave must pass through junctional epithelium layers before echoing off the tooth surface.
(3) A far region with no detectable returns, in which connective tissue completely scatters the ultrasonic wave and no echoes from the tooth can be detected.

Using this model as guide, an idealized two-dimensional periodontium was developed for use in a computer simulation designed to test this model. The simulation was designed using the elastodynamic variation of the CAFIT algorithm, called the elastodynamic finite integration technique.[41] This idealized periodontium consists of three regions: the periodontal pocket, which is filled with water from the ultrasonographic probe, the junctional epithelium, and the gingiva. The inner surface is an interface with the tooth, and so for this lateral boundary the rigid-body boundary condition was used. The outer surface is an interface between gingiva and the oral cavity (air), and so for this lateral boundary the vacuum boundary condition was used.

In addition, the ultrasonic parameters of the gingiva and the junctional epithelium needed to be defined. Because diagnostic ultrasound is not used now in dentistry, values for the Lamé parameters λ and μ were not available in the literature, or for the density ρ. However, because the gingiva contains fiber bundles that give it some stiffness (like muscle), while the junctional epithelium is softer and more skinlike, the ultrasonic properties of skeletal muscle and skin, respectively, were used for this simulation. For muscle, the values $\lambda = 2.46 \times 10^9$ Pa, $\mu = 0.25 \times 10^6$ Pa, and $\rho = 1.08 \times 10^3$ kg/m^3 were used, and for skin, $\lambda = 2.30 \times 10^9$ Pa, $\mu = 0.19 \times 10^6$ Pa, and $\rho = 1.02 \times 10^3$ kg/m^3 were used.[42,43] In the simulations that follow, it should be kept in mind that muscle and skin are probably more dense than gingiva and the junctional epithelium, respectively, since gingiva is softer than muscle and junctional epithelium mixes with crevicular fluid to make it more liquidlike than skin.

The simulation was first run for the case in which the surface of the tooth was completely smooth, and the only return was from the bottom of the simulation space at four reduced distance units (which corresponds to a return at eight reduced time units).

Next, a surface irregularity 0.15 r.u. wide and deep was added to the tooth 1 r.u. down from the top of the periodontium. In this case, a strong primary echo occurs at 2 r.u. (time), with weaker secondary echoes at 4 and 6 r.u. The large echo at 8 r.u. in Fig. 6 is from the bottom of the simulation space.

After completing these initial simulations, another level of complexity was added by accounting for attenuation within the different materials. For the purposes of this simulation, it is assumed water does not attenuate the signal at all over the propagation distances of interest, while the junctional epithelium has a small attenuation factor of 0.999 per simulation step, and gingiva attenuates signals more strongly (due to the presence of collagen fibers) at 0.98 per simulation step. As a result of attenuation, the return off the bottom of the simulation space was eliminated, while the return off the 0.15 r.u. surface irregularity remained. If the surface feature is moved beneath the junctional epithelium to 1.7 r.u., the echoes are still evident, but if it moved further down into the connective tissue of the gingiva, attenuation of the signal is too great for an echo to return to the transducer.

Finally, another simulation was run with the surface feature at 1.7 r.u., but with the junctional epithelium moved from 1.5 to 2.0 r.u. Thus, the irregularity is at the same depth

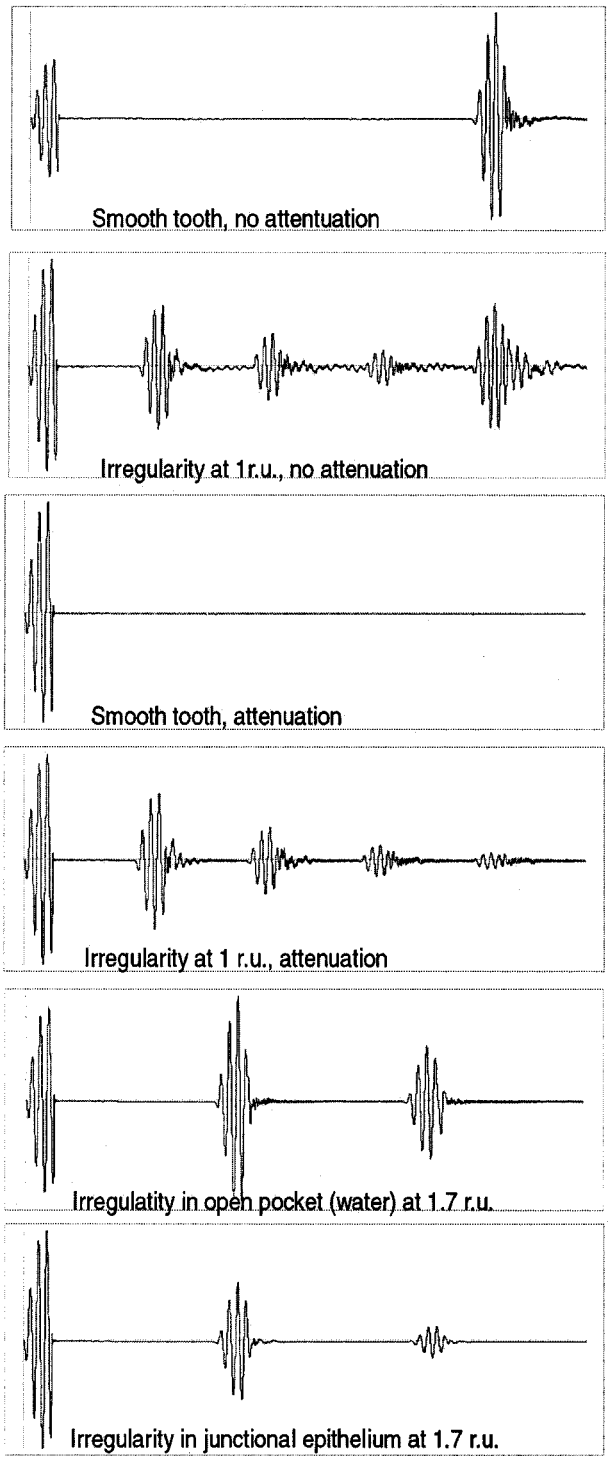

FIG. 6. Traces from a series of simulations of ultrasonic wave propagation within the periodontium. For smooth teeth (first and third traces) there is no return, while there is for teeth with slight irregularities on the surface (second, fourth, fifth, and sixth traces). Finally, that return is larger when the irregularity is in the open pocket (fifth trace) vs when it is covered by junctional epithelium tissue (sixth trace).

as in the earlier simulation, but no longer covered by tissue. As a result, the signal amplitude is higher. The traces produced from these simulations can also be seen in Fig. 6.

From this series of simulations, it appears plausible that return signals in the clinical data are solely the result of echoes from the tooth surface. Since the material properties of the junctional epithelium and the gingiva are not known, it is still possible that ultrasonic echoes could result from interactions with these structures, even though the simulation did not produce such echoes. However, since muscle and skin are most likely more dense than gingiva and junctional epithelium, and therefore more likely to produce echoes, this possibility does not seem likely.

Based on the results of this simulation, it appears likely that transitions in signal strength can be correlated to anatomic features. The first transition from strong peaks to weaker peaks is likely to correspond to the border between the open pocket (or sulcus) and the junctional epithelium, while the second transition from weaker peaks to ''noise'' is likely to correspond to the border between the junctional epithelium and connective tissue.

The ultimate accuracy of this device in a clinical setting will depend on the signal processing algorithms that automatically identify those features in the ultrasonic echoes that correspond to the anatomical features of interest. Our current work is directed towards developing improved versions of these algorithms along with testing the instrument in a variety of clinical settings.

ACKNOWLEDGMENTS

Support for this work was provided by the National Institute of Dental and Craniofacial Research (No. 1R15DE12851-01 and No. 1R43DE1255701-A2) and by Virginia's Center for Innovative Technology (No. BIO-01-004).

[1] Oral Health in America: A Report of the Surgeon General, National Institute of Dental and Craniofacial Research (2000).
[2] A. D. Haffajee *et al.*, J. Clin. Periodontol. **10**, 257 (1982).
[3] J. F. Tessier *et al.*, J. Periodontol. **65**, 103 (1994).
[4] P. S. Hull, V. Clerehugh, and A. Ghassemi-Aval, J. Periodontol. **66**, 848 (1995).
[5] T. E. Rams and J. Slots, Int. J. Periodontal Res. **13**, 521 (1993).
[6] N. P. Lang and E. F. Corbet, Int. Dent. J. **45**, 5 (1995).
[7] G. Greenstein and I. Lamster, J. Periodontol. **66**, 659 (1995).
[8] M. A. Listgarten, J. Clin. Periodontol. **7**, 165 (1980).
[9] L. Tupta-Veselicky, P. Famili, F. J. Ceravolo, and T. Zullo, J. Periodontol. **65**, 616 (1994).
[10] M. E. Palou, M. J. McQuade, and J. A. Rossman, J. Periodontol. **58**, 262 (1987).
[11] F. Hunter, Int. Dent. J. **44**, 557 (1994).
[12] L. Mayfield, G. Bratthall, and R. Attstrom, J. Clin. Periodontol. **23**, 76 (1996).
[13] M. K. Jeffcoat, Scientific **84**, 18 (1991).
[14] M. Quiryen, A. Callens, D. van Steenberghe, and M. Nys, J. Periodontol. **64**, 35 (1993).
[15] M. Cattabriga, Int. Dent. J. **43**, 109 (1993).
[16] S. G. Grossl, R. G. Dunford, H. A. Koch, E. E. Machtei, and R. J. Genco, J. Periodontal Res. **31**, 330 (1996).
[17] D. S. Barendregt, U. van der Velden, J. Relker, and B. G. Loos, J. Clin. Periodontol. **23**, 397 (1996).
[18] J. J. Garnick and L. Silverstein, J. Periodontol. **71**, 96 (2000).
[19] S. F. Wang *et al.*, J. Periodontol. **66**, 38 (1995).
[20] J. F. Tessier *et al.*, J. Clin. Periodontol. **20**, 41 (1993).
[21] L. Tupta-Veselicky *et al.*, J. Periodontol. **65**, 616 (1994).
[22] M. Cattabriga, Int. Dent. J. **43**, 109 (1993).
[23] M. C. K. Yang *et al.*, J. Clin. Periodontol. **19**, 306 (1992).
[24] N. Ahmed, T. L. P. Watts, and R. F. Wilson, J. Clin. Periodontol. **23**, 452 (1996).
[25] A. Aguero *et al.*, J. Periodontol. **66**, 184 (1995).
[26] J. F. Tessier *et al.*, J. Clin. Periodontol. **18**, 548 (1993).
[27] J. G. Keagle *et al.*, J. Clin. Periodontol. **22**, 953 (1995).

[28] S. Albalat *et al.*, Proc. SPIE **3034**, 106 (1997).
[29] M. C. Juan *et al.*, Comput. Med. Imaging Graph. **23**, 209 (1999).
[30] A. D. Hafajee, S. S. Socransky, and J. M. Goodson, J. Clin. Periodontol. **10**, 298 (1983).
[31] W. P. Dreyer *et al.*, Int. Dent. J. **43**, 557 (1993).
[32] C. H. Gibbs, J. W. Hirschfeld, and J. G. Lee, J. Clin. Periodontol. **15**, 137 (1988).
[33] P. F. van der Stelt, Adv. Dent. Res. **7**, 158 (1993).
[34] M. K. Jeffcoat, J. Periodontol. **63**, 367 (1993).
[35] E. Hausmann, J. Clin. Periodontol. **21**, 128 (1994).
[36] M. J. Goodson, J. Clin. Periodontol. **9**, 472 (1982).
[37] E. Hausmann, J. Periodontol. **71**, 497 (2000).
[38] A. Peiffer, B. Kohler, and S. Petzold, J. Acoust. Soc. Am. **102**, 697 (1997).
[39] H. K. Versteeg, *An Introduction to Computational Fluid Dynamics: The Finite Volume Method* (Longman Scientific and Technical, San Francisco, 1995).
[40] Galactic Industries Corp., http://www.galactic.com/algorithms/peak_picking.htm. (2000).
[41] P. Fellinger, R. Marklein, K. J. Langenberg, and S. Klaholz, Wave Motion **21**, 47 (1995).
[42] E. L. Madsen, H. J. Sathoff, and J. A. Zagzebski, J. Acoust. Soc. Am. **74**, 1346 (1983).
[43] S. A. Goss, R. L. Johnston, and F. Dunn, J. Acoust. Soc. Am. **64**, 423 (1978).